The 9th European Congress on Computational Methods in Applied Sciences and Engineering
ECCOMAS Congress 2024
3–7 June 2024, Lisboa, Portugal

A MEMS DEVICE INTEGRATING A METAPLATE FOR VIBRATION ABSORPTION

David Faraci[1], Valentina Zega[1], Gabriele Gattere[2] and Claudia Comi[1]

[1] Department of Civil and Environmental Engineering, Politecnico di Milano
piazza Leonardo da Vinci 32, 20133 Milan, Italy
e-mail: david.faraci@polimi.it, valentinza.zega@polimi.it, claudia.comi@polimi.it

[2] STMicroelectronics, 20007 Cornaredo, Italy
email: gabriele.gattere@st.com

Key words: locally resonant material, metaplate, wave propagation, band gap, MEMS

Summary. The functioning of Micro-Electro-Mechanical Systems based on resonant elements can be severely affected by unwanted external vibrations. In this work, we propose to isolate a MEMS resonator from external disturbances around its driven frequency through a metamaterial plate, integrated in the same device. Transmission and dynamic analyses show the absorption properties of the metaplate and assess the advantage of the proposed solution.

1 INTRODUCTION

In the last decades, Micro-Electro-Mechanical Systems (MEMS) have attracted a lot of interest due to their small size, low-cost batch production, high performances and wide range of applications [1, 2]. Many devices, such as resonant accelerometers or frequency-modulated gyroscopes, are driven at resonance and their functioning relies on the measurement of frequency variation [3, 4, 5, 6]. Vibrations induced by the exterior environment may significantly affect the functioning of such devices [7].

Several solutions are available in the literature to reduce the effects of accidental vibrations [8]. The most common one makes use of differential sensing that allows to cancel, in an ideally perfect structure, the common-mode vibrations effect. Other strategies, effective when the frequency of external vibrations is far from that of the device, make use of signal filtering techniques.

Locally resonant metamaterials (LRM) could represent a possible solution to isolate real MEMS devices (always exhibiting small geometric imperfections) from unwanted external vibrations with frequency close to that of functioning. These media are usually constructed by the periodic repetition of a unit cell, with a resonant part, that allows damping out elastic waves in some frequency ranges called band gaps [9]. Many LRM have been already proposed in the literature [10, 11, 12], but their use in MEMS is limited as their fabrication is hardly compatible with the microlithography processes employed in MEMS [2].

In [13] the authors propose a metamaterial plate, compatible with microlithographic processes, to be employed for the vibration isolation of a MEMS device. The numerical analyses and the experimental tests reported in[14], with the MEMS device and the metaplate fabricated separately and then assembled, show the absorption properties of the LRM plate, even if some local resonance modes appear. These modes arise due to the defect of periodicity in the central part where the MEMS is glued.

In this work, we propose a new device in which an isolating LRM plate and a MEMS resonator are integrated and fabricated together. The LRM plate has a new microstructure with hexagonal unit cells, optimised to filter vibrations around the driving frequency of the resonator. Exploiting the potentialities of a recent fabrication process of STMicroelectronics called "THELMA-Double" (THick Epitaxial Layer for Micro-gyroscopes and Accelerometers) [15], in the proposed design the MEMS resonator is hanging on the metamaterial plate, between the substrate and the plate. This allows the allocation of electrodes to keep unchanged the periodicity of the metaplate and, therefore, improves the absorption of external vibrations. Numerical analyses confirm the good absorption properties of the proposed device to isolate a resonator from external vibrations.

2 MEMS DESIGN

The device proposed in the present work can be fabricated exploiting the recent "THELMA-Double" fabrication process, which mainly consists of the following steps: i) deposition of a sacrificial layer on the substrate; ii) epitaxial growth and etching of a first polysilicon layer (EPI1); iii) deposition of a second sacrificial layer on EPI1 and iv) epitaxial growth and etching of a second polysilicon layer (EPI2). Thus, after the release of sacrificial layers, such a technique allows the manufacturing of MEMS devices with two structural polysilicon layers.

The proposed device contains a LRM plate fabricated on the layer EPI2 of 8 μm thickness, shown in the top view of Figure 1a, which is attached to the substrate at its four corners. The metaplate is composed of a connected region (the matrix) and has periodically arranged hexagonal resonant masses attached to the matrix by three folded springs, as shown in the close-up view of the regular hexagonal cell of side $a = 70$ μm depicted in Figure 1b.

The resonator shown in Figure 1c is fabricated on the layer EPI1 of 20 μm thickness and is located between the substrate and the periodic plate, in the region indicated by the orange box in Figure 1a. The resonator is not anchored to the substrate but it is hanging below the metaplate. The blue-shaded region of Figure 1c represents the portion of the resonator that is attached to the matrix of the above metamaterial plate. The transversal section $s - s$ of the device is shown in Figure 1d (not in scale with the real geometry).

Note that, the proposed layout configuration allows the positioning of electrodes for the in-plane drive and sense of the resonator, indicated in green in Figures 1c and 1d, without the need of cutting the metaplate. If the resonator is fabricated instead on a layer above the metaplate, the latter must be perforated to allow the growth of the electrodes from the substrate to the resonator. This would destroy the periodicity of the metamaterial plate and would not allow us to obtain the desired properties in terms of wave absorption.

The material of the whole device is modeled as isotropic linear-elastic characterized by Young's modulus $E = 148$ GPa, Poisson's ratio $\nu = 0.22$ and mass density $\rho = 2330$ kg/m^3. Numerical analyses are carried out with the commercial finite element software COMSOL Multiphysics using prismatic quadratic serendipity finite elements.

2.1 Resonator

The resonator is clamped in the center and the in-plane in-phase bending mode occuring at 170 kHz, shown in Figure 2 on the left, is considered. Note that the in-phase driving mode, instead of the usually exploited out-of-phase one, is selected to better assess the function of the

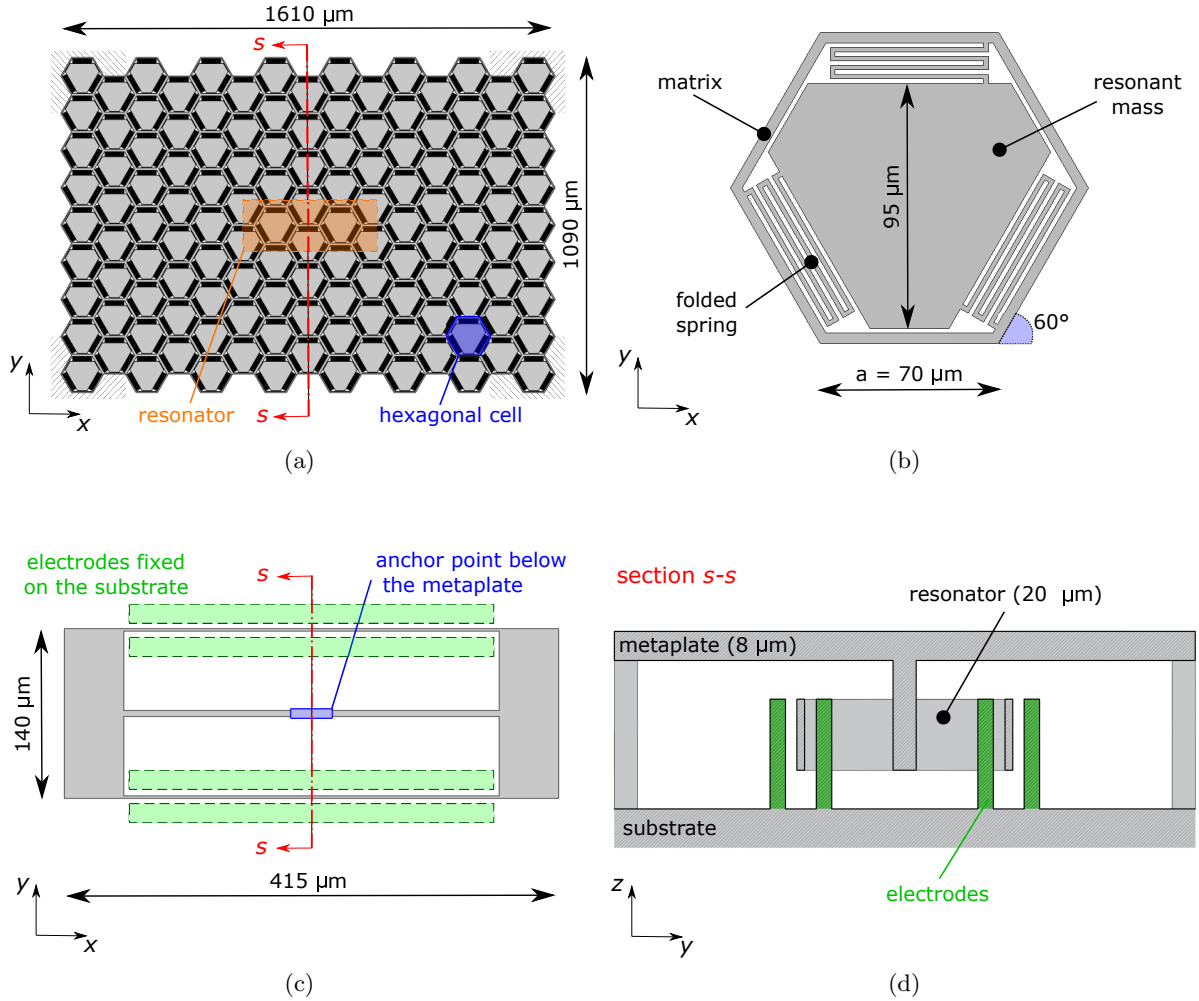

Figure 1: (a) Top view of the metaplate; (b) geometry of the hexagonal cell of the metaplate; (c) geometry of the resonator and (d) transversal section of the device (not in scale).

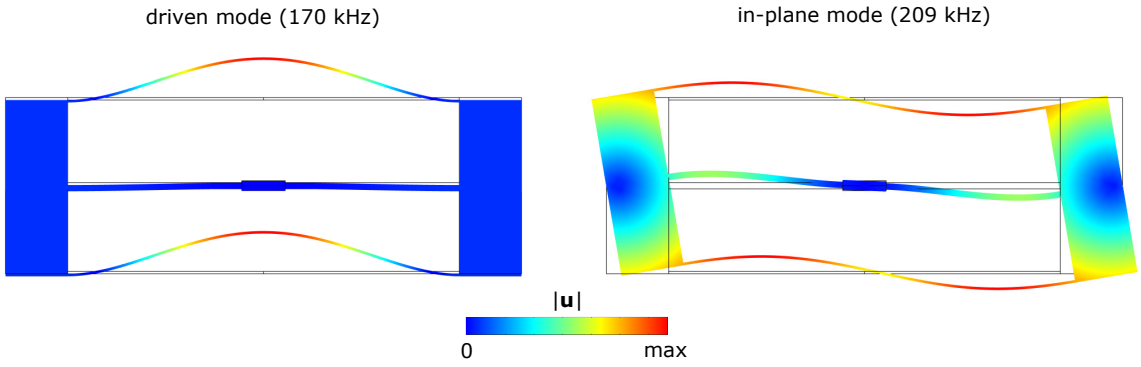

Figure 2: Contours on the deformed shape of displacement magnitude for the chosen driven mode at 170 kHz (left) and the in-plane mode at 209 kHz (right).

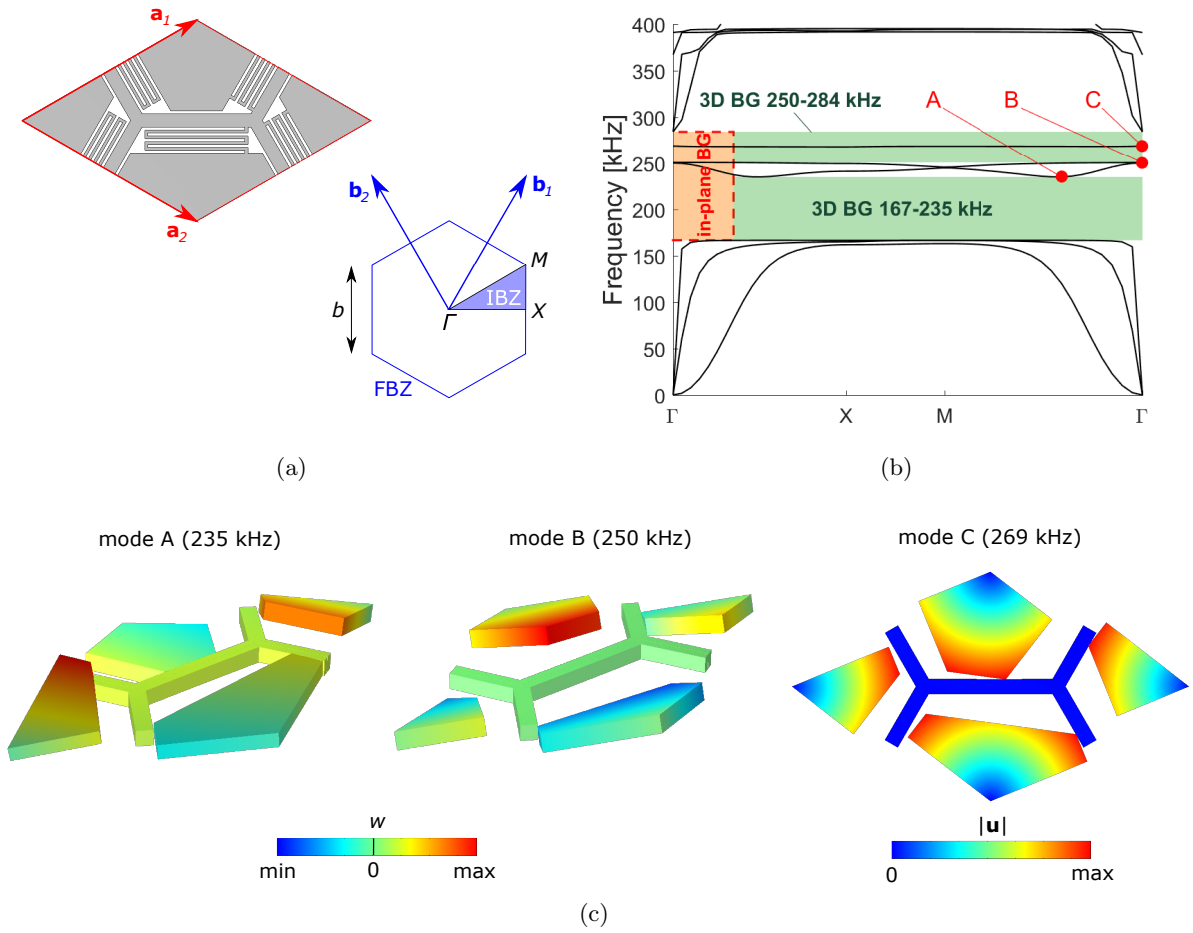

Figure 3: (a) Primitive cell and First Brillouin Zone of the metaplate; (b) dispersion plot of the metaplate; (c) eigenmodes corresponding to points A (left), B (middle) and C (right) in subfigure (b). Folded springs are not displayed for clarity.

proposed device since it is more sensitive to an external vibration.

Figure 2, on the right, shows the subsequent in-plane eigenmode of the resonator, which occurs at 209 kHz.

2.2 Metaplate

The proposed metamaterial plate is characterized by a hexagonal periodicity, which implies that it can be constructed by the periodic repetion of the primitive cell shown in Figure 3a (left) by the primitive vectors

$$\mathbf{a}_1 = a\left(\frac{3}{2}\mathbf{e}_x + \frac{\sqrt{3}}{2}\mathbf{e}_y\right) \qquad \text{and} \qquad \mathbf{a}_2 = a\left(\frac{3}{2}\mathbf{e}_x - \frac{\sqrt{3}}{2}\mathbf{e}_y\right), \tag{1}$$

where $\mathbf{e}_x$ and $\mathbf{e}_y$ are, respectively, the unit vectors of the $x-$ and $y-$axis. The First Brillouin Zone of the plate is shown on the right of the same figure: it is a regular hexagon of side

$b = 4\pi/3a\sqrt{3}$ which is constructed from the reciprocal vectors $\mathbf{b}_1$ and $\mathbf{b}_2$ satisfying the duality conditions

$$\mathbf{a}_i \cdot \mathbf{b}_j = 2\pi\delta_{ij} \qquad \text{for } i, j \in \{1, 2\}, \tag{2}$$

where δ_{ij} is the Kronecker's symbol.

The band structure of the metamaterial plate is reconstructed through Bloch-Floquet numerical analysis [9]. Figure 3b shows the dispersion curves of the designed primitive cell along the edges of the Irreducible Brillouin Zone, i.e., the triangle $\Gamma - X - M$ highlighted in blue in Figure 3a. Frequency intervals where a solution does not exist for any wavevector are highlighted in green. These intervals, also known as band gaps, represent the frequency ranges in which elastic waves cannot propagate without being attenuated in the metamaterial.

For the considered cell, above the first three modes (two in-plane modes and one out-of-plane mode), a complete band gaps opens at 167 kHz.

If one computes the dispersion curves for in-plane polarized waves only, one finds the existence of an in-plane band gap (shaded in orange) between 167 kHz and 284 kHz. However, when considering the full three-dimensional problem, two out-of-plane vibration modes appear in the band structure of the metaplate, resulting in the splitting of the in-plane band gap into two three-dimensional band gaps. Figure 3c (left and middle) shows these two out-of-plane modes for wave vectors corresponding to points A and B indicated in Figure 3b; the contours of the out-of-plane displacement w are represented on the deformed configuration (folded springs are not displayed for clarity).

In the second three-dimensional band gap of the metamaterial plate, it can be observed the presence at 269 kHz of a flat mode. Figure 3c shows the contour of the displacement magnitude of this mode in Γ, from which it can be recognized a rigid rotation of the resonant masses.

Note that the metamaterial plate has been designed such that the driven mode of the resonator to be isolated (Figure 2 on the left) falls inside the first band gap.

3 NUMERICAL ANALYSES

The band gap prediction obtained through Bloch-Floquet analyses discussed in Section 2.2 are valid in the hypothesis of an infinite metamaterial plate having the primitive cell shown in Figure 3a. Since the device proposed in this work has finite dimensions and the metamaterial plate is constrained at its four corners, we perform transmission and transient analysis to assess the real absorption properties of the metaplate for the isolation of the resonator around its driven frequency.

3.1 Transmission analyses

We first compute the response of the whole device when the anchors of the metaplate are subject to an imposed harmonic displacement of 1 μm amplitude, applied along the $x-$, $y-$ or $z-$ direction, in the frequency range between 160 kHz and 240 kHz. With reference to Figure 4a, we evaluate the displacement magnitude at the interface between the resonator and the metaplate (blue marker) and at the mid-span of the resonator beam (red marker) for each one of the three analysis.

Figures 4b, 4c and 4d show in a semi-logarithmic plot the transmission, i.e., the ratio between the evaluated displacement magnitude and the 1 μm imposed displacement, in the three cases considered.

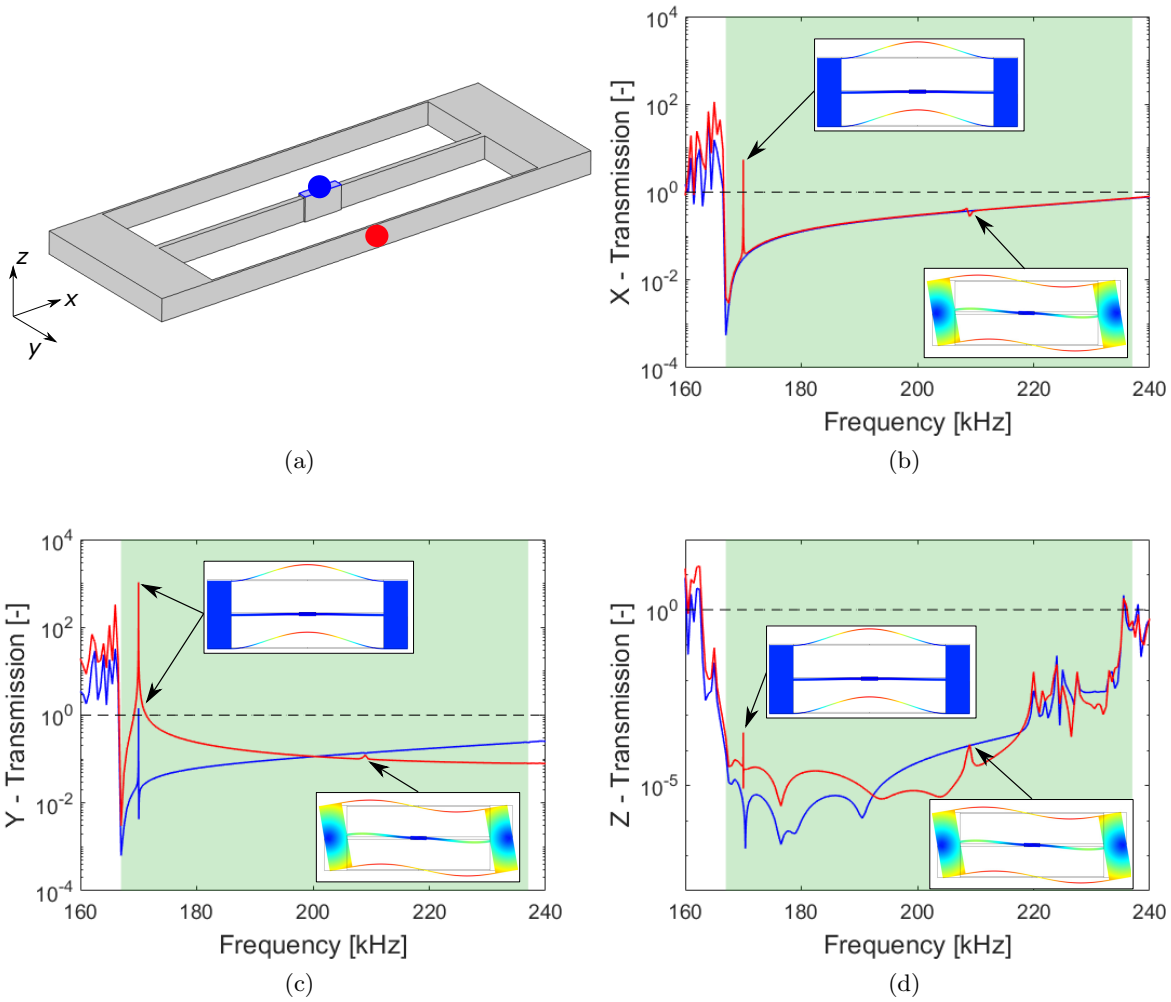

(a) (b) (c) (d)

Figure 4: (a) 3D view of the resonator. Transmission curves in the case of: (a) $x-$, (b) $y-$ and (c) $z-$ imposed displacement at the metaplate anchors.

As it is possible to see from the in-plane transmissions (Figures 4b and 4c), the displacement at the anchor point of the resonator (blue curve) and the one at the beam mid-span (red curves) are remarkably attenuated in the whole band gap, except at the driven frequency of the resonator (170 kHz) where the transmission curves exhibit a peak. A further peak, of very small amplitude, can be observed within the band gap at the frequency of the other in-plane mode of the resonator (see Figure 2, right).

Similar comments apply for the out-of-plane transmission analysis (Figure 4d), with the difference that a sequence of peaks appears in the band gap starting from 220 kHz. These peaks are associated with local out-of-plane eigenmodes of the metamaterial plate which are due to its dimension and to the prescribed boundary conditions. However, their presence do not affect the functioning of the resonaotr since they occur at frequencies much higher than the driving one of the resonator.

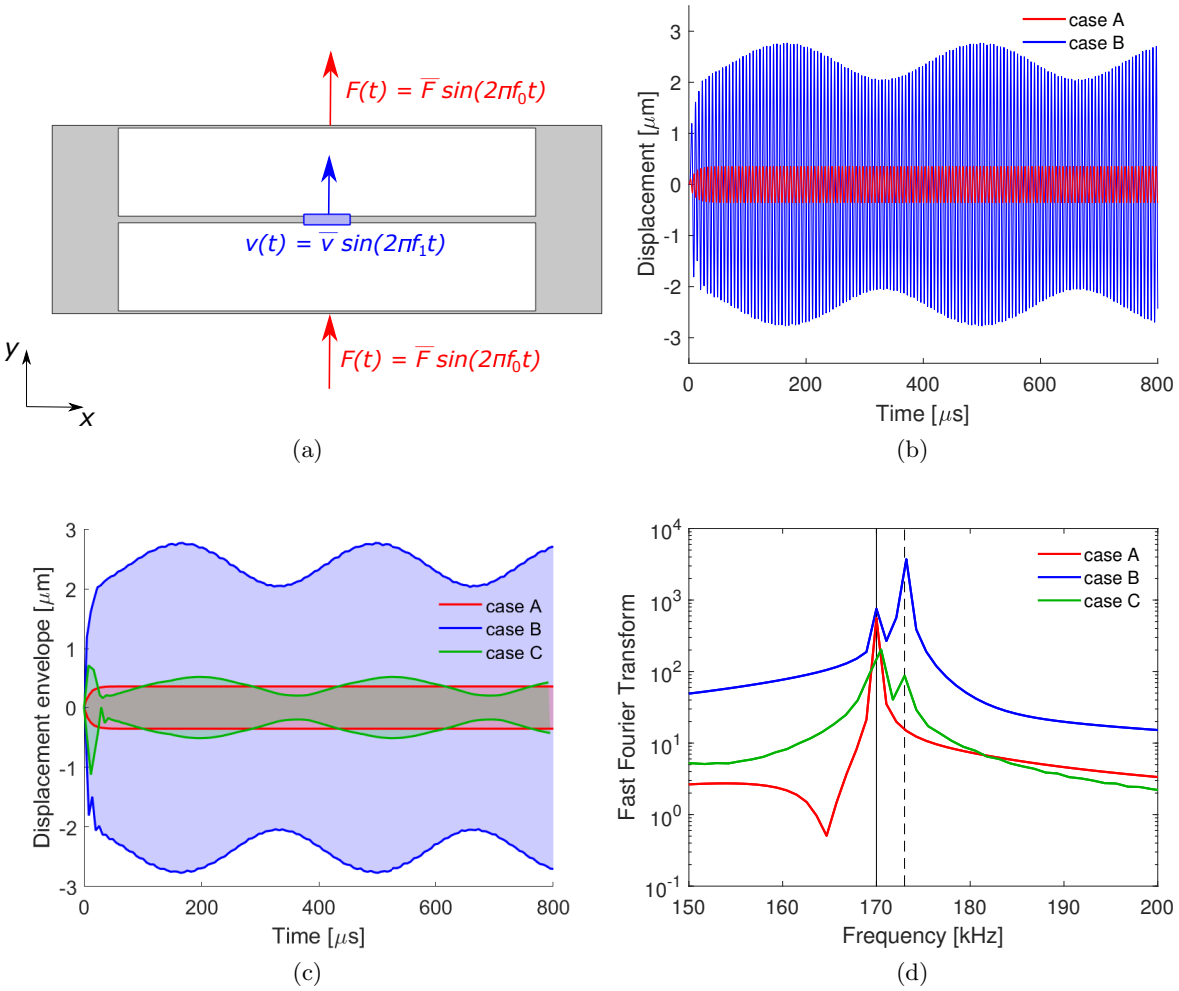

Figure 5: (a) Loading condition of the resonator in case B; (b) Time history of the resonator displacement in cases A and B; (c) displacement envelope and (d) Fourier transforms of the responses in the three cases.

3.2 Transient analyses

To further study the isolation properties of the proposed device, we simulate the dynamic response of the actuated resonator subject to an external vibration with and without the LRM metaplate. The dynamic analyses are carried out with a high damping ratio $\xi = 0.1$ to rapidly damp out the transient response and reach the steady-state regime.

We compare three different scenarios. In the first one (case A) the resonator is actuated with the forces $F(t) = \overline{F}\sin(2\pi f_0 t)$ applied at the beam midspan, as shown in Figure 5a, with $\overline{F} = 1$ μN and $f_0 = 170$ kHz being the driven frequency.

In case B the resonator is actuated and considered anchored directly to the substrate, thus any external vibration are transferred to it through its anchor point (see the blue region in Figure 5a). We consider, as an example, an external imposed displacement $v(t) = \overline{v}\sin(2\pi f_1 t)$

along the $y-$axis of amplitude $\overline{v} = 1$ μm at a frequency $f_1 = 173$ kHz, close to f_0.

The comparison between the responses of these first two cases can be observed by the time evolution of the beam mid-span displacement shown in Figure 5b. The oscillations of the actuated resonator subjected to the external vibration (case B, blue curve) are magnified with respect to the purely actuated one (case A, red curve) and exhibit the beating phenomena.

The third case (C) corresponds to the proposed solution where the metaplate is employed. In this case, the external vibration $v(t)$ is applied to the anchors of the plate (see Figure 1a) and it is damped by the local resonant mechanisms before reaching the resonator, which is hanging below the central region of the plate.

Figure 5c compares the envelope of the displacement magnitude in the three different cases considered. As it is possible to see, with the solution proposed in the present work (case C), the amplitude of vibration of the resonator is comparable with the actuated one without external vibrations (case A). Even if the beating phenomena can still be observed, these results confirm that the metamaterial plate allows to strongly reduce the disturb caused by external vibrations (compare the magnitudes of the response in cases B and C).

A further comparison can be performed if one looks at the Fourier's transform of the steady-state time evolution in a neighborhood of the drive frequency. In all three cases, a peak can be observed in correspondence of the frequency f_0 (solid black line) at which the resonator is actuated. When an external vibration with a frequency f_1 (dashed black line) is considered (cases B and C), a second peak in the signal can be detected, but its magnitude is significantly lower when the solution with the metaplate is adopted (case C).

4 CONCLUSIONS

In this work, we propose the use of a locally resonant metaplate to isolate a resonator from external vibrations. In particular, we design a MEMS device composed by a LRM metamaterial plate, bound to the substrate, and a mechanical resonator which is hanging below the metaplate. The metamaterial plate is designed to have a band gap around the driven frequency of the resonator. The proposed layout configuration, with the resonator between the substrate and the plate, is feasible thanks to the "Thelma-Double" process, it enables the simultaneous integrated fabrication of the MEMS and of the metaplate, and it allows for the presence of drive and sense electrodes withouth altering the periodicity of the metaplate.

Transmission analyses show the effective absorption that the proposed device provides in a frequency range close to the eigenfrequency of the resonator actuated mode. Finally, we perform dynamic analyses to compare the response of a classical MEMS resonator, attached to the substrate, with the one obtained using the filtering metaplate, for an imposed external vibration. The results show clearly a strong reduction of the disturbance in the oscillation of the resonator, therefore attesting the potentialities of the proposed solution.

REFERENCES

[1] Corigliano, A., Ardito, R., Comi, C., Frangi, A., Ghisi, A., Mariani, S. *Mechanics of Microsystems*, Wiley (2018).

[2] Vigna, B., Ferrari, P., Villa, F.F., Lasalandra, E., Zerbini, S., *Silicon Sensors and Actuators.* Springer (2022).

[3] Acar, C., Shkel, M. *MEMS Vibratory Gyroscopes: Structural Approaches to Improve Robustness*. Springer-Verlag (2008).

[4] Keshavarzi, M., Hasani, J.Y. Design and optimization of fully differential capacitive MEMS accelerometer based on surface micromachining. *Microsyst. Technol.* **25**(4), pp. 1369-1377 (2019).

[5] Song, Y., Panas, R.M., Hopkins, J.B. A review of micromirror arrays. *Precis. Eng.* **15**, pp. 729-761 (2018).

[6] Beek, J.T.M., Puers, R. A review of MEMS oscillators for frequency reference and timing applications. *J. Micromech. Microeng.* **22**(1) (2012).

[7] Agarwal, M. *et al.* Effects of mechanical vibrations and bias voltage noise on phase noise of MEMS resonator based oscillatiors. In: *Proc. 19th IEEE Int. Conf. Micro electro Mech. Syst.*, pp. 154-157 (2006).

[8] Yoon, S. W. Vibration isolation and shock protection for MEMS. Ph.D. dissertation, Dept. Elect. Eng. Comput. Sci., Univ. Michigan, Ann Arbor, MI, USA (2009)

[9] Laude, V. *Phononic Crystals*. De Gruyter (2015).

[10] Xiao, Y., Wen, J., Huang, L., Wen, X. Analysis and experimental realization of locally resonant phononic plates carrying a periodic array of beam-like resonators. *J. Phys. D: Appl. Phys.* **47** (2014)

[11] D'Alessandro, L., Zega, V., Ardito, R., Corigliano, A.. 3D auxetic single material periodic structure with ultra-wide tunable bandgap. *Sci. Rep.* **8** (2018)

[12] Faraci, D., Comi, C., Marigo, J.J. Band gaps in metamaterial plates: asymptotic homogenization and Bloch-Floquet approaches. *J. Elas.* ***148*** *(2022).*

[13] Yao, Z., Zhao, R., Zega, V., Corigliano, A., A metaplate for complete 3D vibration isolation. *Eur. J. Mech.-A/Solids* **84** (2020).

[14] Yao, Z., Zega, V., Su, Y., Zhou, Y., Ren, J., Zhang, J., Corigliano, A. Design, Fabrication and Experimental Validation of a Metaplate for Vibration Isolation in MEMS. *Journal of Microelectromechanical System* **29**(5) (2020).

[15] Vercesi, F., Corso, L., Allegato, G., Gattere, G., Guerinoni, L., Valzasina, C., Nomellini, A., Alessandri, A., Gelmi, I. THELMA-Double: a new technology platform for manufacturing of high-performance MEMS inertial sensors. In: *Proc. 35th IEEE Int. Conf. Micro electro Mech. Syst.*, pp. 778-781 (2022).